

Biodistribution Properties of ^{111}In -labeled C-Functionalized *trans*-Cyclohexyl Diethylenetriaminepentaacetic Acid Humanized 3S193 Diabody and $\text{F}(\text{ab}')_2$ Constructs in a Breast Carcinoma Xenograft Model

Kiki Tahtis, Fook-Thean Lee, Fiona E. Smyth, Barbara E. Power, Christoph Renner, Martin W. Brechbiel, Lloyd J. Old, Peter J. Hudson, and Andrew M. Scott¹

Tumor Targeting Program, Ludwig Institute for Cancer Research, Melbourne Branch, Austin and Repatriation Medical Centre, Victoria 3084, Australia [K. T., F.-T. L., F. E. S., C. R., A. M. S.] and CRC for Diagnostic Technologies and CSIRO Division of Health Sciences and Nutrition [B. E. P., P. J. H.], Victoria 3052, Australia; Radioimmune and Inorganic Chemistry Section, Radiation Oncology Branch, DCS, National Cancer Institute, NIH, Bethesda, Maryland 20892 [M. W. B.]; and Ludwig Institute for Cancer Research, New York Branch, Memorial Sloan Kettering Cancer Center, New York, New York 10021 [L. J. O.]

ABSTRACT

The humanized complementarity determining region-grafted anti-Lewis Y (Le^y) monoclonal antibody [humanized 3S193 (hu3S193)] was developed for targeting Le^y -expressing epithelial tumors such as breast, colon, lung, prostate, and ovarian carcinoma. We are exploring the potential use of smaller molecular size, bivalent analogues of hu3S193, because the faster blood clearance of $M_r \sim 54,000$ diabody and $M_r \sim 110,000$ $\text{F}(\text{ab}')_2$ molecules may be advantageous in achieving optimal and rapid tumor uptake for diagnostic and potential therapeutic applications. The single-chain variable fragment-5 residue linker construct (diabody) was expressed using the bacterial secretion vector pPOW3, and soluble product was purified without refolding processes. The $\text{F}(\text{ab}')_2$ fragment was obtained by pepsin digest of parental hu3S193. To facilitate evaluations, the radiometal ^{111}In was used to label C-functionalized *trans*-cyclohexyl diethylenetriaminepentaacetic acid chelated diabody and $\text{F}(\text{ab}')_2$. The immunoreactivity of the radiolabeled constructs was 41.3 and 58.6%, and the K_a was $1.68 \times 10^6 \text{ M}^{-1}$ and $5.33 \times 10^6 \text{ M}^{-1}$ for the diabody and $\text{F}(\text{ab}')_2$, respectively. Radioconjugates were injected into mice bearing Le^y -positive MCF-7 tumors, and biodistribution properties were determined at various time points after injection. The up-

take of radiolabeled diabody in xenografts was maximal at 1 h after injection ($4.7 \pm 0.6\%$ injected dose/g), whereas the $\text{F}(\text{ab}')_2$ peaked at 8 h after injection ($14.2 \pm 2.4\%$ injected dose/g). The tumor:blood ratio at 4 h for the diabody and $\text{F}(\text{ab}')_2$ was 5:1 and 2:1, which increased to 20:1 and 5:1, respectively, at 8 h and increased further to 40:1 and 130:1, respectively, at 48 h. These results demonstrate that the diabody construct may have applications as a diagnostic imaging reagent, whereas $\text{F}(\text{ab}')_2$ displayed effective tumor targeting and may have potential as a therapeutic molecule in patients with Le^y -expressing tumors.

INTRODUCTION

Carcinoma of the breast is the most common malignancy affecting female patients and is the second most frequent cause of death from cancer (1). Although an increasing number of cases are surgically cured as a result of early diagnosis and effective systemic adjuvant chemotherapy, some patients present with advanced disease, and many others develop recurrent and/or metastatic cancer. These patients may be palliated using a variety of treatments including hormonal and cytotoxic therapy; however, response is usually temporary, and it is difficult to demonstrate prolongation of survival (2). In view of this, efforts to identify new active drugs and treatment regimens continue. Conventional radiotherapy and chemotherapy target both normal and neoplastic cells, relying upon the enhanced sensitivity of rapidly dividing cancer cells to achieve preferential killing (3). In contrast, mAb² constructs can be directed more specifically against tumor-associated antigens, which may be expressed on the surface of the tumor cells (4).

A number of tumor antigens have been shown to have high expression on malignant breast cancer cells, including HER2/neu, MUC, CEA, and Le^y (5). Le^y is a member of the H-type II blood group-related antigens and is a difucosylated tetrasaccharide that is carried on both glycoproteins and glycolipids, with chemical structure $\text{Fuc}\alpha 1 \rightarrow 2\text{Gal}\beta \rightarrow 4(\text{Fuc}\alpha 1 \rightarrow 3)\text{GlcNAc}$ (6). The Le^y antigen is located on the epithelial cell surface and is expressed in >70% of epithelial cancers including breast, prostate, pancreatic, colon, ovary, and lung cancer. Expression is also observed on 60% of endometrial and gastric carcinomas (7–9). The Le^y tumor-associated antigen is an attractive target

Received 6/7/00; revised 11/20/00; accepted 1/10/01.

The costs of publication of this article were defrayed in part by the payment of page charges. This article must therefore be hereby marked *advertisement* in accordance with 18 U.S.C. Section 1734 solely to indicate this fact.

¹ To whom requests for reprints should be addressed, at Ludwig Institute for Cancer Research, Austin and Repatriation Medical Centre, Heidelberg, Victoria 3084, Australia. Phone: (613) 9496-5876; Fax: (613) 9496-5892; E-mail: ams@austin.unimelb.edu.au.

² The abbreviations used are: mAb, monoclonal antibody; Le^y , Lewis y; CEA, carcinoembryonic antigen; p.i., post injection; hu3S193, humanized 3S193; scFv, single chain variable fragment; %ID/g, percentage injected dose/gram; FPLC, fast performance liquid chromatography; CHX-A'-DTPA, C-functionalized *trans*-cyclohexyl diethylenetriaminepentaacetic acid; CDR, complementarity determining region.

for immunotherapy because it is broadly applicable to many types of carcinomas, its expression is homogeneous in both primary and metastatic lesions, and there is high antigen density on the tumor cell surface (6, 8). The parental 3S193 mAb was produced using standard hybridoma technology after immunization of BALB/c nude mice with Le^y-expressing MCF-7 breast cancer cells. 3S193 has been humanized (hu3S193) by CDR grafting, and reactivity for Le^y was confirmed to be similar to the murine version (10). Recent studies have extended these early studies and confirmed that hu3S193 can be produced and formulated on a large scale as a potential immunotherapeutic reagent against selected solid tumors (11).

This report explores the use of new smaller molecular weight multivalent analogues of the parent hu3S193 antibody. Antibody fragments including F(ab')₂ and scFv molecules such as diabody and triabodies [in which the variable heavy (V_H) and variable light (V_L) regions of the construct are stabilized by a flexible linker], are advantageous in that they offer improved clinical pharmacokinetics because of their smaller size and their reduced immunogenicity (because of the absence of an Fc domain; Refs. 12–14). They may also have more homogeneous tumor penetration, which may circumvent problems of inaccessibility/poor penetration into the tumor mass, and display improved specific tumor retention associated with multivalency (4, 15, 16). However, their rapid clearance from the blood often results in a lower absolute uptake in the tumor (15, 17–19). Hence, these smaller molecules are often more suitable for diagnostic imaging, rather than as therapeutic reagents, particularly because their rapid clearance from background tissue permits early imaging of patients/tumors after administration of the radioconjugate. In this study, the bivalent diabody and F(ab')₂ versions of hu3S193 were characterized *in vitro* for their binding, affinity, and stability properties. The *in vivo* biodistribution of the ¹¹¹In-CHX-A''-DTPA-labeled hu3S193 diabody and F(ab')₂ was also evaluated using a BALB/c nude mouse breast carcinoma xenograft model to ascertain their potential in targeting Le^y-expressing solid tumors.

MATERIALS AND METHODS

Cell Lines and Antibodies

MCF-7, a Le^y-expressing human breast adenocarcinoma cell line (20), was obtained from American Type Culture Collection (Rockville, MD). SW1222, a Le^y-negative human colonic cancer cell line, was obtained from the New York branch of the Ludwig Institute. Both MCF-7 and SW1222 cells were cultured in RPMI supplemented with 10% FCS (CSL Biosciences, Melbourne, Victoria, Australia) and 50 units/ml penicillin-streptomycin (Life Technologies, Inc., Grand Island, NY). The hu3S193 mAb was obtained from the Biological Production Facility (Ludwig Institute for Cancer Research, Melbourne, Victoria, Australia; Ref. 11).

scFv- 5 Diabody Production

The heat-inducible bacterial expression vector (pPOW3) was used to synthesize diabodies into the periplasm of *Escherichia coli* Top 10 cells (Invitrogen, Carlsbad, CA) according to conditions described previously (21, 22). In brief, the hu3S193 diabody comprised two identical scFv molecules in which V_H

and V_L domains were linked via a five-amino acid residue (Gly₄Ser) linker. A FLAG octapeptide affinity tag (DYKD-DDDK) at the COOH terminus of the V_L domain assisted with protein purification. Diabody production was performed in 10 liter fermenter batches; the cells were then harvested by centrifugation at 4°C for 5 min at 6000 × *g* and then stored frozen at –80°C. The pellet was thawed and processed to yield a soluble periplasmic protein fraction of ~3 liters. For hu3S193, the protocol produced 1 mg/liter of purified, soluble diabody of the expected size (*M_r* ~54,000) with <1% of higher molecular weight aggregates detectable by HPLC size exclusion chromatography.³ The hu3S193 diabody could be stored frozen at 1 mg/ml and thawed without aggregation in Immunopure Gentle Ag/Ab Elution Buffer (Pierce, Rockford, IL).

F(ab')₂ Digestion and Purification

The parental hu3S193 mAb (10 mg/ml) was digested by incubation with pepsin (Sigma Chemical Co., St. Louis, MO) in 0.2 M sodium acetate buffer (pH 3.5). The digestion was performed at room temperature for 2 h using an optimal antibody:pepsin ratio of 200:1. After digestion, the reaction mixture was neutralized to pH 7.0 with 1 M NaOH. Antibody purification was performed using Protein A-Sepharose affinity chromatography (Amersham Pharmacia, Uppsala, Sweden), followed by size exclusion chromatography on a Sephacryl S-200 column (Amersham Pharmacia) to separate the F(ab')₂ fragments. The purified protein was concentrated using a YM30 Amicon ultrafiltration membrane (Amicon, Beverly, MA) to a concentration of 5.4 mg/ml. Protein purity was assessed by SDS-PAGE and FPLC analyses.

Chelation and Radiolabeling

Proteins were radiolabeled either directly with ¹²⁵I or via a bifunctional metal ion chelating agent, CHX-A''-DTPA, for ¹¹¹In. Antibody constructs were labeled with ¹¹¹In (NEN Life Science Products, Boston, MA), using a modification of a method described previously (23). In brief, proteins were placed in 8-mm Spectra/Por cellulose ester membrane (Spectrum, Houston, TX) with a molecular weight cutoff of 10,000 and dialyzed against 0.1 M borate buffer containing 2.5 g/l of Chelex 100 resin (Bio-Rad, Hercules, CA; pH 8.0) to remove heavy metals. CHX-A''-DTPA was added in a molar excess of 3:1 and incubated at room temperature overnight, protected from light. Excess unbound antibody was removed by dialysis for 8 h with 20 mM sodium acetate buffer containing 0.15 M NaCl (pH 6.4). ¹¹¹In was bound to CHX-A''-DTPA antibody conjugates under mildly acidic conditions (pH 5.5) for 20 min, and then the pH was raised to 7.0 by the addition of small aliquots of 2.0 M sodium acetate, followed by 10 mM EDTA for quenching unbound ¹¹¹In. The radiolabeled mixture was purified by centrif-

³ B. E. Power, J. M. Caine, J. E. Burns, D. R. Shapira, M. K. Hattarki, K. Tahtis, F-T. Lee, F. E. Smyth, A. M. Scott, A. A. Kortt, and P. J. Hudson. Construction, expression, and characterization of a single-chain diabody derived from a humanised anti-Lewis Y cancer targeting antibody using a heat-inducible bacterial secretion vector, in press, Cancer Immunol. Immunother.

ugal desalting on a Sepharose G50 column (Pharmacia, Uppsala, Sweden) equilibrated with PBS. Radioiodination with ^{125}I (NEN Life Science Products, Boston, MA) was performed via a modified chloramine-T reaction (24), using a chloramine T:protein ratio of 4:1. Chloramine-T (Merck, Darmstadt, Germany) was dissolved in 0.5 M potassium phosphate buffer (pH 7.0); after a brief 2-min incubation period, the reaction was terminated by the addition of a 5-fold excess of sodium metabisulfite (BDH Chemicals, Melbourne, Victoria, Australia), again dissolved in 0.5 M potassium buffer. The product was purified through a desalting P6DG column (Bio-Rad) equilibrated in PBS.

Immunoreactivity

The immunoreactive fraction of the radiolabeled constructs with MCF-7 cells was determined according to Lindmo *et al.* (25). Briefly, 20 ng of ^{111}In -CHX-A''-DTPA diabody or $\text{F}(\text{ab}')_2$ were added to an increasing concentration of MCF-7 cells (antigen excess) or SW1222 control cells. The assay was incubated for 45 min at room temperature with continuous mixing to keep the cells in suspension. Cells were washed three times to remove any unbound antibody, and pellets were measured in a dual gamma scintillation counter (Cobra II, Model 5002, Auto-gamma; Packard Instruments, Canberra, Australian Capital Territory, Australia) that is capable of measuring the cpm of two isotopes simultaneously. The percentage of binding of hu3S193 to MCF-7 cells was calculated by the formula: $(\text{cpm cell pellet}/\text{mean cpm of radioactive antibody standards}) \times 100$. Immunoreactivity was obtained by plotting the double reciprocal plot for binding against cell concentration using SigmaPlot for Windows (Jandel Scientific, San Rafael, CA).

Scatchard Assay

Scatchard analysis was used to determine the affinity constant (K_a) and number of antigen binding sites/cell (25). Unlabeled hu3S193, at concentrations ranging from 0.02 to 200 $\mu\text{g}/\text{ml}$, was mixed with 15 ng of labeled ^{111}In -CHX-A''-DTPA diabody or $\text{F}(\text{ab}')_2$. The antibody mixture was added to 15×10^6 MCF-7 cells and incubated for 45 min at room temperature with continuous mixing. Specific binding (X axis) was plotted against the ratio of specific binding to concentration of free radioligand (Y axis). The intercept at the abscissa represented the binding capacity of the cell (antibody molecules bound/cell). The apparent association constant can be derived from the slope of the line. A detailed explanation of the calculations can be obtained from Clarke *et al.* (26).

Serum Stability

Serum stability was assessed by incubating 2 μg of each radiolabeled protein in 200 μl of healthy donor human serum at 37°C for a 5-day period. The radiochemical purity of the samples was analyzed by FPLC analysis at 1, 4, 24, and 48 h after incubation, and single-point immunoreactivity assays at 0 (no incubation), 0.5, 1, 2, 4, 16, 24, and 48 h after incubation, with additional time points of 72, 96, and 120 h after incubation for $\text{F}(\text{ab}')_2$. $\text{F}(\text{ab}')_2$ analysis was extended to 120 h to account for the longer half-life of the molecule.

Single-Point Immunoreactivity Assay. Twenty ng of each radiolabeled construct were incubated with 10×10^6

MCF-7 cells alone or in the presence of 300 μg of competing unlabeled, intact hu3S193 mAb. The 45-min incubation was performed on a rotary mixer at room temperature. Cells were washed three times to remove any unbound antibody, and pellets were measured in a dual gamma scintillation counter (Packard Instruments). Duplicate preincubation radioconjugate standards were measured concurrently with the cell pellet, and binding was expressed as a percentage compared with duplicate preincubation radioconjugate standards.

FPLC Analysis. The constructs were analyzed by FPLC before and after labeling to determine the integrity of the radiolabeled proteins. The samples were eluted isocratically on a Superdex 200 HR10/30 column (Amersham Pharmacia) using 50 mM phosphate, 150 mM NaCl (pH 7.0) at a flow rate of 0.5 ml/min. Eluted radiolabeled antibodies were detected by UV absorbance at 280 nm by a Beckman System Gold detector (Beckman Instruments, Fullerton, CA), and radioactivity was measured by Packard Radiomatic Flo One (Packard Instruments). For serum stability analysis, 60 1-min (0.5-ml fractions) were collected using the Pharmacia Radi-Frac fraction collector (Amersham Pharmacia) on the column described above. The amount of protein in each fraction was detected by UV absorbance at 280 nm using a Life Science UV/Vis Spectrophotometer DU 530 (Beckman Instruments), and radioactivity was measured in a dual gamma scintillation counter (Packard Instruments).

SDS-PAGE Analysis. Transchelation with serum proteins was analyzed by incubating ^{111}In -CHX-A''-DTPA diabody (0.24 μCi radioactivity/4 μg protein) and ^{111}In -CHX-A''-DTPA $\text{F}(\text{ab}')_2$ (2.9 μCi radioactivity/2 μg protein) in normal human serum for 4 h at 37°C. Samples were separated by 4–20% Tris-HCl SDS-PAGE under nonreducing conditions (Bio-Rad) at 200 V for 1 h. Protein bands were visualized with Coomassie blue staining and autoradiography using Hyperfilm MP (Amersham Life Science, Buckinghamshire, England) and image intensifying screens at -70°C .

Animal Model

To establish MCF-7 human breast cancer xenografts, BALB/c nude mice obtained from the Walter and Elisa Hall Institute (Melbourne, Victoria, Australia) were supplemented with exogenous estrogen. A slow release estrogen pellet (0.72 mg of 17 β -estradiol; Innovative Research of America, Sarasota, FL) was implanted s.c. in the scapular region, using a small incision closed by a single stitch using silk 5/0 nonabsorbable sutures (B. Braun Surgical, Melsungen, Germany) at the same time as injection of tumor cells. Mice received 20×10^6 MCF-7 cells s.c. into the left inguinal mammary line, and 2 weeks later, 3×10^6 of the more rapidly dividing SW1222 cells were injected into the right inguinal mammary line (Le y -negative control cell line). The establishment of tumors was monitored by tumor volume measurement $[(L \times W^2)/2]$, where length was the longest axis and width the measurement at right angles to length (26).

Biodistribution Study

Seventy-five mice (a combination of two studies) with a mean \pm SD MCF-7 tumor volume of 457 ± 197 mg were

divided into two groups. All constructs were administered i.v. via the retro-orbital plexus. The first group of 29 mice was injected with ¹¹¹In-CHX-A''-DTPA diabody (total of 5 μg of antibody; 3.9 μCi of radioactivity). The second group of 46 mice received ¹¹¹In-CHX-A''-DTPA F(ab')₂ (total of 1.6 μg of antibody; 3.3 μCi of radioactivity). At the designated time points p.i., groups of mice (*n* = 2–5) were sacrificed by Ethrane anesthesia, mice were bled by cardiac puncture, and tumors and organs [skin, liver, spleen, small intestine, stomach, kidney, brain, bone (femur), lungs, and heart] were resected immediately. All samples were counted in a dual gamma scintillation counter (Packard Instruments). Triplicate standards prepared from the injected material were counted at each time point with tissue and tumor samples enabling calculations to be corrected for the physical decay of the isotopes. Results of the labeled antibody distribution over time were expressed as %ID/g. The tissue distribution data were calculated as the mean %ID/g ± SD for the diabody (*n* = 4) and F(ab')₂ (*n* = 5), per time point.

Whole Body Imaging and Pharmacokinetic Analysis

Imaging. Whole body imaging of mice was performed at 1, 4, and 24 h after radioconjugate injection. Mice were anesthetized at these time points by i.m. injection of 150 mg/kg ketamine (Troy Laboratories, Smithfield, New South Wales, Australia) and 5 mg/kg diazepam (Bayer Australia, Sydney, New South Wales, Australia) and placed under a Trionix Biad gamma camera (Biad Trionix Research Laboratories, Twinsburg, OH). Twenty-min images were obtained at each time point. Images were acquired in a 256 × 256-bit matrix, and a standard of known concentration was included in the field of view.

Pharmacokinetics. Pharmacokinetics (*T*_{1/2α} and *T*_{1/2β}) were determined for ¹¹¹In-labeled radioconjugates using a standard curve-fitting program (SAAM II; University of Washington, Seattle, WA), assuming a four-parameter, two-compartment model to calculate pharmacokinetic results.

RESULTS

Chelation and Radiolabeling

FPLC size-exclusion chromatography showed that both the diabody and F(ab')₂ were stable proteins during freeze/thaw cycles (data not shown). Proteins were thawed when required and radiolabeled separately with ¹¹¹In and ¹²⁵I. Intact hu3S193 was radiolabeled with ¹¹¹In (35.4% labeling efficiency) as a control. The labeling efficiency of the diabody and F(ab')₂ was 14.4 and 44.1% with ¹¹¹In and 5.0 and 50.0% with ¹²⁵I, respectively. The constructs were analyzed by FPLC before (data not shown) and directly after labeling to verify the integrity of the radiolabeled proteins (Figs. 1A and 2A). Only the ¹¹¹In-labeled constructs were used in the biodistribution study.

Immunoreactivity and Affinity Analysis

Immunoreactivity Assay. A Lindmo cell binding assay was performed for each of the immunoconjugates to evaluate their antigen-binding capabilities after radiolabeling. The assay was performed using Le^y-positive MCF-7 breast carcinoma cells, and to assess whether there was any nonspecific binding of the antibody constructs, control Le^y-negative

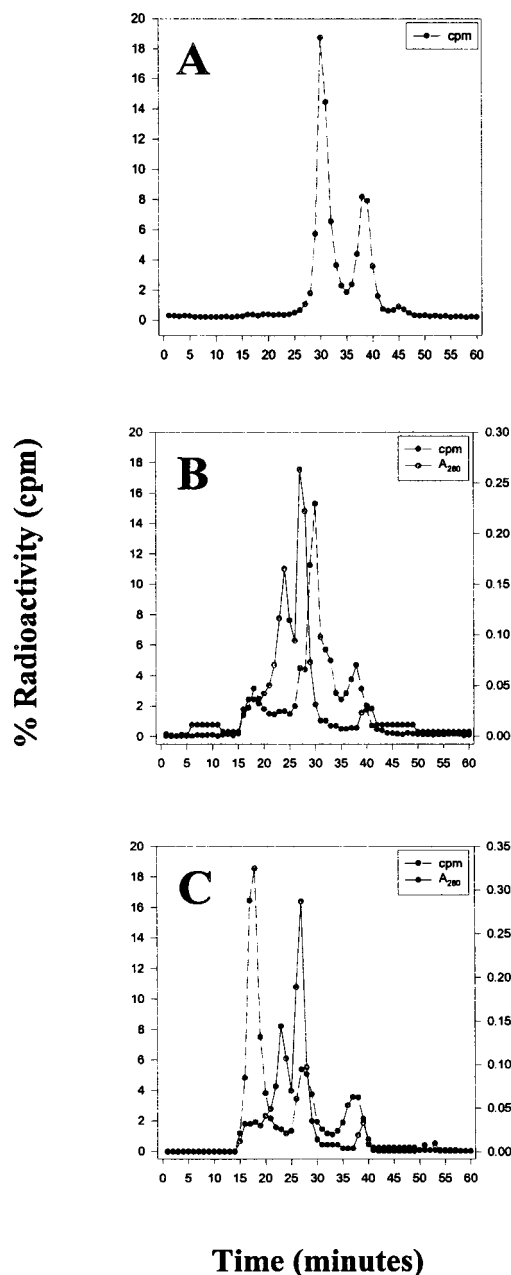


Fig. 1 ¹¹¹In-CHX-A''-DTPA hu3S193 diabody was analyzed by FPLC for its serum stability properties: A, in 5% human serum albumin at 0 h after incubation; B, in normal human serum at 1 h; and C, 48 h after incubation. Protein detected at A₂₈₀ nm is represented by —, whereas radioactivity measured by gamma counting is represented by ----. B and C, the protein peaks represent thyroglobulin (*M*_r 669,000; ~18 min), immunoglobulin (*M*_r 150,000; ~24 min), and human serum albumin (*M*_r 67,000; ~27.5 min), where 1-min fractions were collected.

SW1222 colon carcinoma cells were included. The ¹¹¹In and ¹²⁵I diabody radioconjugate binding curves reached saturation as expected (Fig. 3A). The ¹²⁵I diabody had a 2-fold higher immunoreactivity than its ¹¹¹In-labeled counterpart (83.5% compared with 41.3%; Fig. 3A). The ¹¹¹In and ¹²⁵I

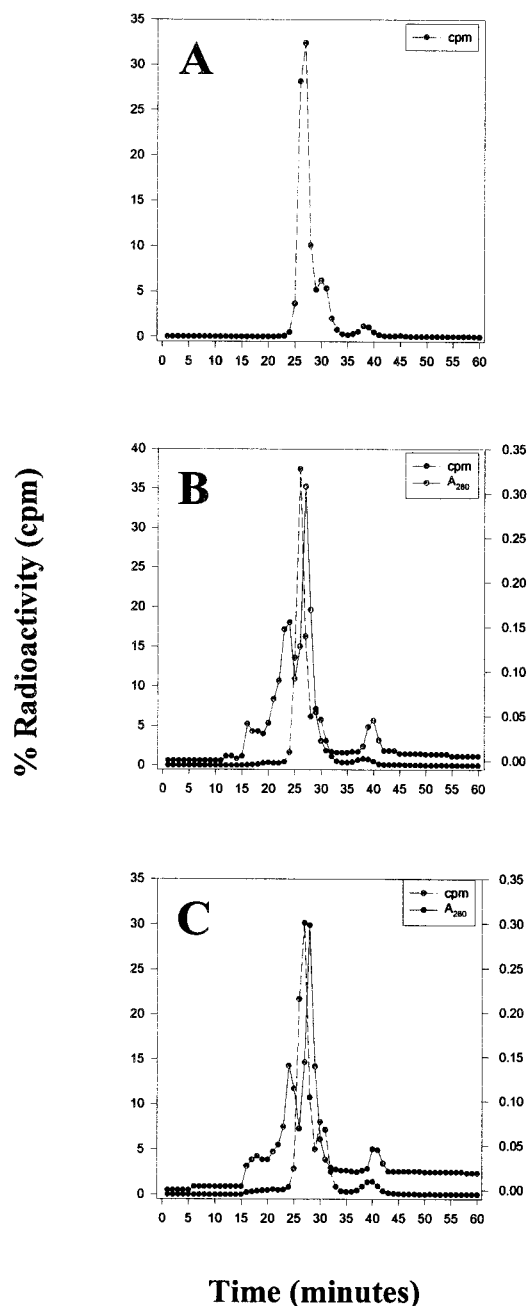


Fig. 2 ¹¹¹In-CHX-A''-DTPA hu3S193 F(ab')₂ was analyzed by FPLC for its serum stability properties: A, in 5% human serum albumin at 0 h after incubation; B, in normal human serum at 1 h; and C, 48 h after incubation. Protein detected at A₂₈₀ nm is represented by —, whereas radioactivity measured by gamma counting is represented by ----. B and C. The protein peaks represent thyroglobulin (*M_r* 669,000; ~18 min), immunoglobulin (*M_r* 150,000; ~24 min), and human serum albumin (*M_r* 67,000; ~27.5 min), where 1-min fractions were collected.

F(ab')₂ binding curves did not appear to reach a plateau and displayed marginally higher immunoreactivity with ¹¹¹In (¹¹¹In, 58.6% and ¹²⁵I, 51.1%; Fig. 3B). No binding to SW1222 cells was observed, indicating that the binding was specific to Le^y antigen (data not shown).

Table 1 Scatchard binding affinities of radiolabeled hu3S193 antibody constructs

	<i>K_a</i> (M ⁻¹) ^a	Binding sites/cell ^b
¹¹¹ In-F(ab') ₂	5.33 × 10 ⁶	1.05 × 10 ⁷
¹²⁵ I-F(ab') ₂	7.93 × 10 ⁶	7.67 × 10 ⁶
¹¹¹ In-diabody	1.68 × 10 ⁶	2.1 × 10 ⁷
¹²⁵ I-diabody	1.30 × 10 ⁶	2.95 × 10 ⁷
¹¹¹ In-intact hu3S193 ^c	1.02 × 10 ⁷	4.62 × 10 ⁶

^a Binding affinity constant for Le^y antigen on MCF-7 breast carcinoma cells.

^b MCF-7 breast carcinoma cells.

^c Data from Clarke *et al.* (26).

Table 2 Serum stability of ¹¹¹In-radiolabeled hu3S193 diabody and F(ab')₂ constructs at 37°C

Time after incubation (h)	Diabody (% bound) ^a	F(ab') ₂ (% bound)
0	26.8	32.0
0.5	17.8	30.1
1	17.5	29.8
2	7.7	28.9
4	4.6	30.1
16	0	30.9
24	0	28.6
48	0	22.8
72	—	21.9
96	—	19.9
120	—	15.9

^a Binding to Le^y-positive MCF-7 cells is expressed as a percentage compared with preincubation radioconjugate standards.

Scatchard Assay. Scatchard analysis was used to calculate the apparent association constant (*K_a*) and number of antigen binding sites/cell (Table 1). The affinity of both the diabody and F(ab')₂ was lower than that of the intact hu3S193 antibody, the affinity of which is within the range expected for binding the Le^y carbohydrate antigen (27). The affinity of the diabody was ~10-fold lower than the parental hu3S193 intact antibody. The F(ab')₂ displayed a slightly higher affinity than the diabody, most likely attributable to the orientation of the binding domains, in addition to the increased stability and immunoreactivity observed for this molecule. The number of binding sites/cell was similar for both constructs.

Serum Stability Analysis

The single-point immunoreactivity assay was used to evaluate the stability of the diabody and F(ab')₂ after incubation in normal human serum for up to 5 days (Table 2). The ¹¹¹In-labeled diabody displayed a gradual reduction in antigen-binding capacity with time. A loss of one-third immunoreactivity was observed within 30 min of incubation in serum, followed by over two-thirds reduction in binding ability at 2 and 4 h after incubation. By 16 h after incubation in serum, all immunoreactivity was lost for the diabody construct. This loss in immunoreactivity correlates with the FPLC chromatographic profiles of the diabody (Fig. 1). FPLC analysis indicated high radiochemical purity of the diabody directly after labeling with ¹¹¹In, with most of the radioconjugate eluting at the expected time of 30

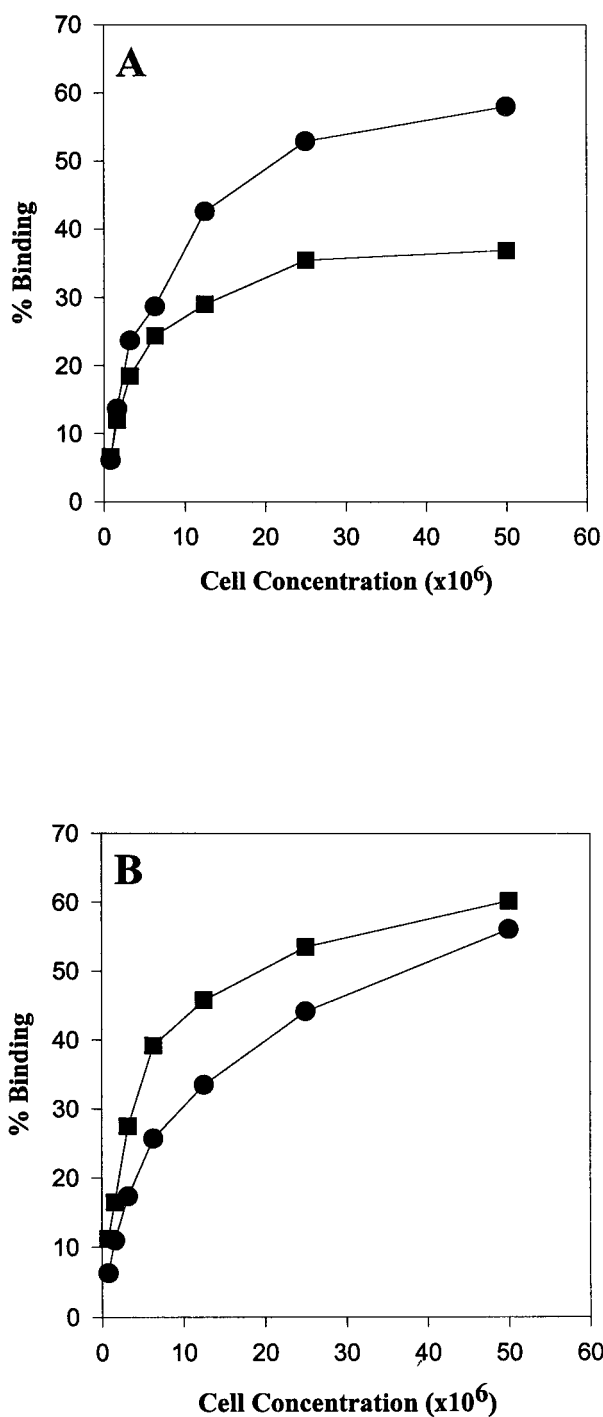


Fig. 3 Lindmo assay for determining the immunoreactivity of ¹²⁵I- (●) and ¹¹¹In-CHX-A''-DTPA (■) diabody (A) and F(ab')₂ (B) with Le^y-positive MCF-7 cells. Immunoreactivity was obtained by plotting the double reciprocal plot for binding against cell concentration.

min (a smaller molecular weight species also appeared to label); however, this was followed by the formation of a high molecular weight aggregate (eluting at 18 min, in a similar position to thyroglobulin). The aggregate was evident as a small peak at 1 h

after incubation (Fig. 1B) but increased markedly by 4 h incubation in serum. After 48 h incubation, most of the diabody was present as the high molecular weight species (Fig. 1C). The ¹¹¹In-labeled F(ab')₂ was more stable in serum. A loss of one-third immunoreactivity was observed between 48 and 96 h after incubation, with a further reduction (50% loss of initial immunoreactivity) observed at 120 h (Table 2). The radiolabeled hu3S193 F(ab')₂ indicated no aggregation, with the majority of ¹¹¹In eluting with F(ab')₂ protein at the expected time of 26 min at all time points investigated (Fig. 2). SDS-PAGE analysis of radiolabeled diabody and F(ab')₂ incubated in serum for 4 h examined the nature of the aggregates further. The radiolabeled constructs were visualized by autoradiography. The radiolabeled diabody migrating as a single band at the expected size of $M_r \sim 30,000$, indicating no transchelation to serum proteins. The F(ab')₂ migrated as a single band at the expected size of $M_r \sim 120,000$, with a minor band also present at $M_r \sim 50,000$, indicating a labeled breakdown product (data not shown).

Biodistribution Study

The *in vivo* targeting potential of the ¹¹¹In-labeled diabody and F(ab')₂ was assessed in BALB/c nude mice bearing MCF-7 Le^y-positive tumors and control SW1222 Le^y-negative tumors. The tumor, blood, and normal tissue retention of each radiolabeled construct was determined at 10 and 30 min and 1, 2, 4, 8, 24, and 48 h, with additional time points of 72 and 96 h for the F(ab')₂. The diabody study was only extended to 48 h because of the very fast clearance of this construct, which had been observed in preliminary experiments. After injection, the diabody displayed a rapid equilibration phase ($T_{1/2\alpha}$, 0.45 h) and subsequent slower elimination phase ($T_{1/2\beta}$, 2.7 h) from the circulation; the F(ab')₂ displayed slightly longer elimination ($T_{1/2\alpha}$, 1.76 h) and equilibration ($T_{1/2\beta}$, 12.6 h) phases (Fig. 4). In contrast, specific and prolonged localization of the radioconjugates to the Le^y-expressing MCF-7 tumor was observed as demonstrated by the tumor:blood ratios (Table 3) and the blood clearance and tumor localization (Figs. 4–6; Table 3). Maximal uptake of radiolabeled diabody in the MCF-7 experimental tumor was seen at 1 h p.i., $4.7 \pm 0.6\%$, whereas the F(ab')₂ peaked at 8 h p.i., $14.2 \pm 2.4\%$ ID/g. Binding to the control SW1222 tumor was negligible for both constructs (Figs. 4–6). The biodistribution analysis of both conjugates showed high kidney uptake (Figs. 5 and 6), without significant localization to the other normal tissues investigated (Figs. 5 and 6).

Imaging

Localization of ¹¹¹In-labeled diabody and ¹¹¹In-labeled F(ab')₂ to MCF-7 tumors in BALB/c nude mice over time is presented in Figs. 7 and 8. At 1 h p.i., no tumor localization was evident for either of the constructs, with the image showing generalized blood pool activity. By 4 and 24 h p.i., minimal uptake was observed in the control tumor, but definite specific localization of radioconjugate was observed in the MCF-7 xenograft for both of the constructs. Some cardiac blood pool activity and kidney uptake was also observed at these time points (Figs. 7 and 8).

DISCUSSION

Recombinant scFv, multivalent molecules, and antibody fragments are emerging as promising new molecules for poten-

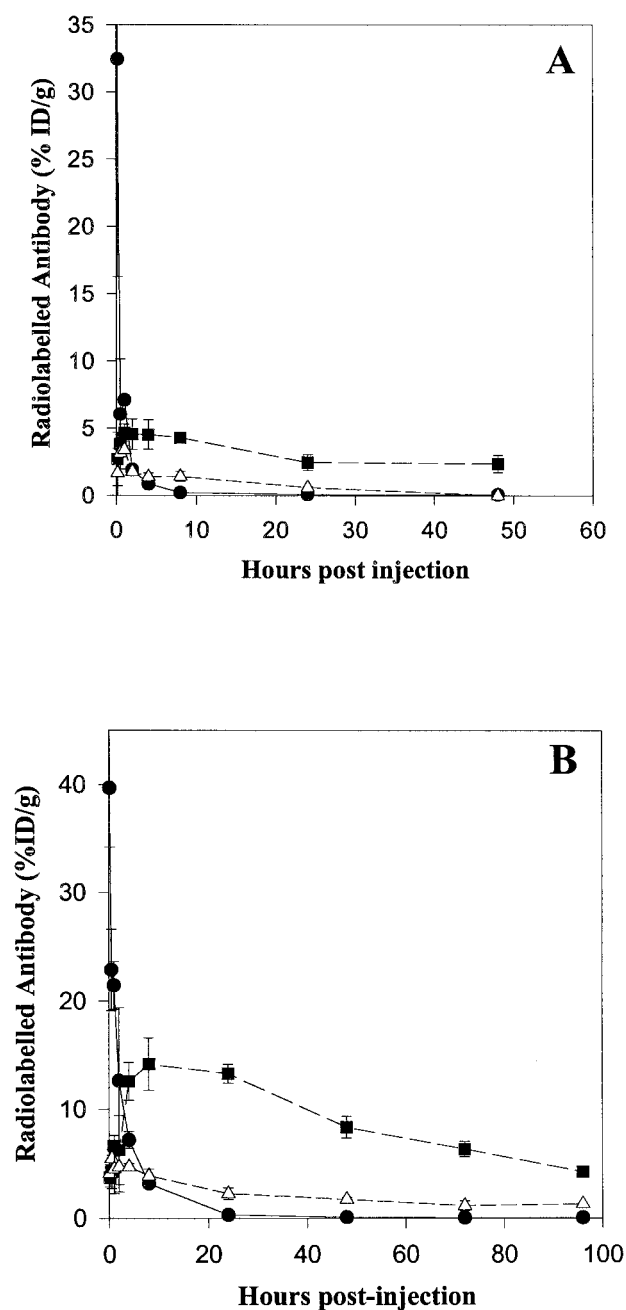


Fig. 4 The blood clearance and tumor localization of the ^{111}In -CHX-A''-DTPA huS193 diabody (A) and F(ab')₂ (B) in blood (●), MCF-7 (■), and SW1222 (△) tumors at time points p.i. Data, mean %ID/g for groups of $n =$ two to five mice; bars, SD.

tial use in tumor diagnosis and therapy (17, 28, 29). These constructs have a number of important features, including a smaller size that may permit more effective and homogeneous tumor penetration, increased avidity and retention time of antigen:antibody interaction associated with multivalency, and a potentially reduced immunogenicity (18, 30, 31). However, they also demonstrate a rapid clearance from the circulation, resulting in a low absolute tumor uptake, and the *in vivo* behavior of

the new construct designs remains to be fully established (15, 32, 33). The purpose of this study was to evaluate the potential of radiolabeled diabody and F(ab')₂ constructs of the humanized antibody huS193 and to determine the *in vivo* behavior and targeting potential to Le^y-expressing human breast carcinoma xenografts. Both constructs were characterized for their *in vitro* binding, affinity, and stability properties, as well as their *in vivo* biodistribution and pharmacokinetic characteristics. No prior study has rigorously examined diabody and F(ab')₂ constructs concurrently in the same tumor model.

The differences observed in the radiolabeling efficiency between the diabody and F(ab')₂ constructs may be attributable to the reduced number of accessible lysine and tyrosine residues present in the smaller huS193 diabody molecule. The scFv of huS193 contains seven lysine residues as potential sites for chelation and labeling with ^{111}In , compared with ~100 residues found in the intact antibody. A lysine residue is located in CDR two of both the variable heavy and light chains. Binding of CHX-A''-DTPA chelate at these sites may have contributed to the decreased binding capacity of the diabody. Hence, site-directed mutagenesis experiments are planned in an attempt to improve the labeling efficiency of the ^{111}In -labeled diabody compared with the iodinated diabody construct. Additional lysine residues are planned to be inserted at the NH₂ or COOH terminus, or alternatively lysines will be substituted in the binding domains to avoid potential obstruction during the chelation process.

The differences seen in the immunoreactivity between the two isotopes may be attributable to the nature of the constructs and the different ways in which these isotopes are catabolized within the cell. Furthermore, the Scatchard results show a slightly decreased affinity for the diabody compared with the intact and F(ab')₂ huS193 (Table 1), and the lower affinity may reduce the immunoreactivity of the diabody (29, 34). The *in vitro* plasma stability analysis of the diabody indicated that there was loss of stability with time, with a complete loss in immunoreactivity observed by 16 h incubation at 37°C (Table 2), and the subsequent formation of a larger molecular weight species observed by FPLC (Fig. 1, B and C). However, given the fast serum clearance of this construct ($T_{1/2\beta}$, 2.7 h; Fig. 4A), the stability and immunoreactivity of the diabody at 4 h p.i. and beyond may not be as critical. This is also supported by the gamma camera images obtained at 4 and 24 h p.i. for this construct (Fig. 7). The F(ab')₂ retained its immunoreactivity for a longer period of time (120 h), without any apparent degradation or aggregation being observed (Fig. 2). The stability of the bond between the CHX-A''-DTPA chelate and the ^{111}In radio-metal has been rigorously investigated previously (23, 35–37), and the FPLC and binding data for the F(ab')₂ stability analysis suggest that transchelation of the isotope does not occur, because the majority of the radioisotope elutes with the antibody construct. SDS-PAGE analysis demonstrated no transchelation of ^{111}In from the chelated huS193 diabody construct to serum proteins (results not shown), indicating that the aggregates observed by FPLC analysis were not attributable to transchelation.

^{111}In was selected for the *in vivo* biodistribution study because of the higher labeling efficiency observed compared with ^{125}I , its suitability for gamma camera imaging because of its favorable gamma emissions (173 and 247 keV), and its

Table 3 MCF-7 xenograft %ID/g tumor uptake and tumor:blood (T:B) ratios for the ¹¹¹In-CHX-A''-DTPA diabody and F(ab')₂

Time after injection	¹¹¹ In-Diabody % ID/g (mean ± SD) ^a	¹¹¹ In-Diabody (T:B)	¹¹¹ In-F(ab') ₂ % ID/g (mean ± SD)	¹¹¹ In-F(ab') ₂ (T:B)
10 min	2.71 ± 2.0	1:12	3.71 ± 0.9	1:11
30 min	3.83 ± 0.6	1:2	4.23 ± 1.6	1:5
1 h	4.67 ± 0.6	1:2	6.64 ± 1.0	1:3
2 h	4.55 ± 1.1	2:1	6.26 ± 3.2	1:2
4 h	4.52 ± 1.1	5:1	12.59 ± 1.8	2:1
8 h	4.30 ± 0.3	20:1	14.18 ± 2.4	5:1
24 h	2.46 ± 0.6	30:1	13.30 ± 0.9	55:1
48 h	2.36 ± 0.7	40:1	8.37 ± 1.0	127:1
72 h	—	—	6.36 ± 0.7	178:1
96 h	—	—	4.27 ± 0.4	83:1

^a % ID/g was calculated. Data are presented as mean ± SD.

shorter half-life, which complements the rapid clearance of the constructs (38). Hence, the ¹²⁵I isotope was inappropriate for this study, particularly as we were evaluating the ability of the diabody molecule for potential as a diagnostic imaging reagent. It is important that isotope selection is tailored to match the clearance of the antibody. A recent study using ²¹³Bi CHX-A''-DTPA conjugated to an anti-HER2/neu diabody illustrated that the physical half-life of ²¹³Bi (47 min) was too short for optimal pairing with the diabody, resulting in a lack of demonstration of specific uptake in the tumor (39). In contrast, other scFv studies involving longer lived isotopes such as ¹²³I and ⁹⁰Y demonstrated a greater specific tumor accumulation (18, 40, 41). In addition, ¹¹¹In was selected because superior tumor targeting was observed previously with the intact hu3S193 antibody labeled with ¹¹¹In-CHX-A''-DTPA compared with the ¹²⁵I-labeled construct in the same MCF-7 xenograft mouse model used for the diabody and F(ab')₂ experiments (30.1 ± 4%ID/g with ¹¹¹In-labeled hu3S193 compared with 10 ± 3.9%ID/g for ¹²⁵I-labeled hu3S193 at 48 h p.i.; Ref. 26). Preliminary experiments have also indicated that the hu3S193 mAb is internalized into MCF-7 cells and directed to the lysosomes (data not shown), as has been reported with other murine antibodies directed to the same antigen (42). Therefore, a radiometal such as ¹¹¹In, which is trapped within the lysosomal compartment after endocytosis, is a more desirable choice of isotope than ¹²⁵I, which is extruded rapidly from the cell (43).

The *in vitro* studies were extended to a comprehensive *in vivo* biodistribution study, using an established Le^y-positive breast cancer xenograft model in BALB/c athymic nude mice (26). The blood clearance was very rapid for the ¹¹¹In-labeled diabody, and specific localization of the radioconjugate was greater to the Le^y-expressing MCF-7 tumor compared with control SW1222 tumor (Figs. 4–6). Maximum tumor uptake for the hu3S193 diabody was observed at 1 h p.i. (4.7 ± 0.6%ID/g). Investigations with ¹²³I-labeled anti-CEA (8-amino acid linker) and ¹²³I-labeled anti-HER2/neu (5-amino acid linker) diabodies reported maximal tumor uptake at 2 h p.i. (13.68 ± 1.49%ID/g) and 4 h p.i. (10.1%ID/g), respectively (18, 30). The higher xenograft uptake observed in these two studies may reflect the higher affinity of these constructs, as determined by surface plasmon resonance (K_a of the anti-CEA diabody, $8.19 \times 10^{10} \text{ M}^{-1}$; K_a of the anti-HER2/neu diabody, $4 \times 10^{10} \text{ M}^{-1}$) and the lower affinity associated with antigens such as Le^y (K_a of

hu3S193 diabody, $1.68 \times 10^6 \text{ M}^{-1}$). The low uptake of radio-labeled diabody in tumor xenografts may also be explained by the stability properties of this construct in serum, which indicated a rapid loss in binding accompanied by the formation of a large molecular weight aggregate between 0 and 4 h after incubation. The hu3S193 F(ab')₂ displayed similarly quick serum clearance and MCF-7 tumor-specific uptake (Figs. 4B and 6), also illustrated by the high resolution gamma camera images acquired at 4 and 24 h p.i. (Fig. 8). Maximal tumor uptake for the F(ab')₂ was observed at 8 h p.i. ($14.2 \pm 2.4\% \text{ID/g}$). This agrees with other studies investigating F(ab')₂ molecules, which reported similar or lower uptake. A study by Brown *et al.* (44), evaluating an anti-B72.3 F(ab')₂ labeled with both ¹²⁵I and ¹¹¹In, observed maximal uptake at 6 h p.i. for both radioconjugates (¹²⁵I, $8.74 \pm 1.7\% \text{ID/g}$; ¹¹¹In, $10.4 \pm 1.8\% \text{ID/g}$). Two other studies with anti-CEA F(ab')₂ constructs observed greatest uptake in tumor xenografts at 12 h p.i. [$11.1 \pm 2.3\% \text{ID/g}$ (LoVo cells) and $11.2 \pm 3.2\% \text{ID/g}$ (Co112 cells); Ref. 45] and at 6 h p.i. ($12.8\% \text{ID/g}$; Ref. 19).

Tumor uptake of diabody was observed through 48 h p.i. (2.36% ID/g), and high levels of F(ab')₂ in tumors were observed for the 96 h of study (4.27% ID/g). The excellent tumor:blood ratios reflect the specific retention of both constructs in the target tumor and avidity of the constructs for the Le^y antigen (Table 3). At 4 h p.i., the tumor:blood ratios for the genetically engineered hu3S193, anti-CEA (18), and anti-HER2/neu (30) diabody constructs were 5:1, 5.8:1, and 1.5:1, respectively, and increased to 30:1, 48.7:1, and 9.5:1 at 24 h p.i., respectively. The tumor:blood ratio for the F(ab')₂ at 4 h p.i. was 2:1 and increased to 55:1 at 24 h p.i.; this result is impressive when compared with other F(ab')₂ molecules. For example, Pedley *et al.* (19) observed a tumor:blood ratio of 3.7:1 at 24 h p.i., whereas Vogel *et al.* (45) reported tumor:blood ratios ranging from 3.3 ± 0.3 : 1 for LoVo cells and 3.8 ± 0.2 : 1 for Co112 cells in similar studies involving an anti-CEA F(ab')₂ construct. Our results are favorable in comparison with these other studies, particularly in view of the reduced binding avidity associated with antigens such as Le^y (27). The pharmacokinetic results also concur with the biodistribution observations illustrating a rapid terminal clearance from the blood.

The pharmacokinetic properties observed for the hu3S193 diabody and F(ab')₂ constructs in this study are highly comparable with other reports investigating diabody and F(ab')₂ mol-

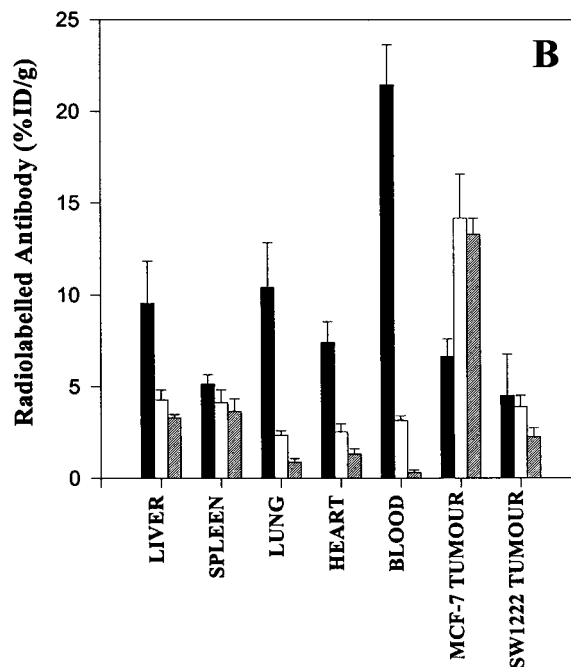
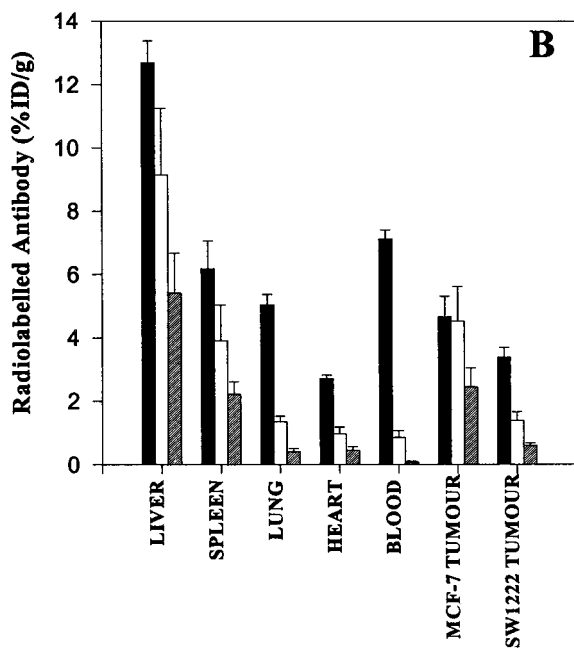
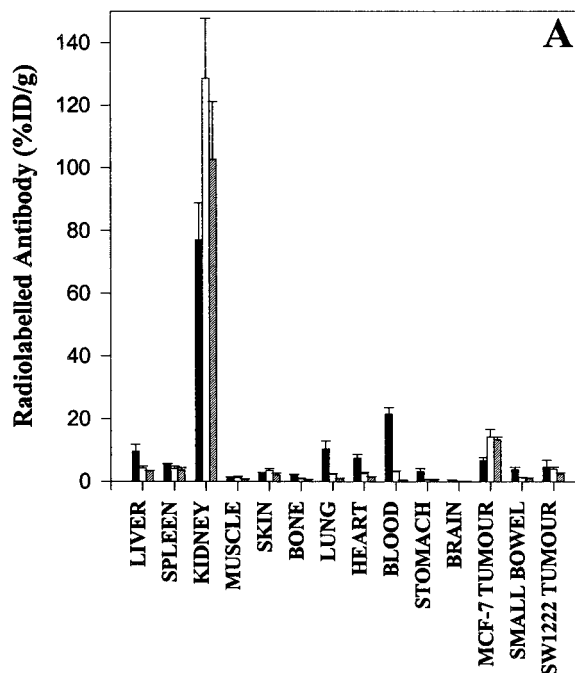
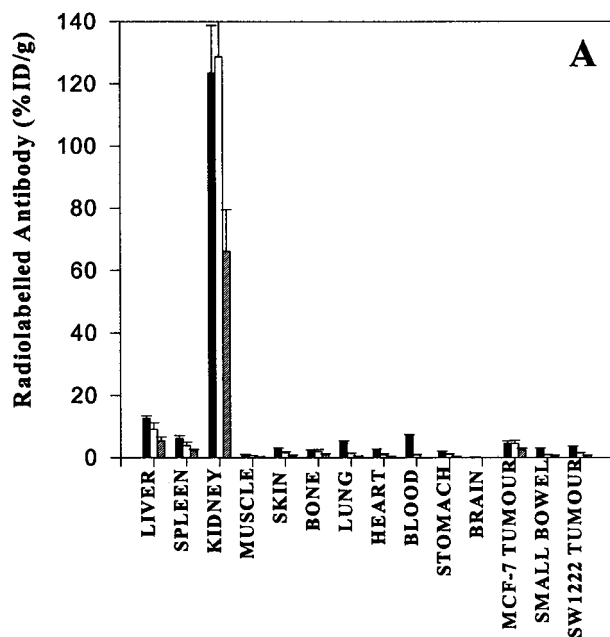


Fig. 5 Biodistribution of ¹¹¹In-CHX-A''-DTPA hu3S193 diabody in groups of *n* = 4 BALB/c nude mice bearing Le^y-positive MCF-7 and control SW1222 tumors. Identical data from 1 h (■), 8 h (□), and 24 h (▨) p.i. is presented in A and B, expressed as mean %ID/g; bars, SD. The kidney data are not included in B, thereby allowing a smaller %ID/g scale and closer examination of the biodistribution data.

Fig. 6 Biodistribution of ¹¹¹In-CHX-A''-DTPA hu3S193 F(ab')₂ in groups of *n* = 5 BALB/c nude mice bearing Le^y-positive MCF-7 and control SW1222 xenografts. Identical data from 1 h (■), 8 h (□), and 24 h (▨) p.i. is presented in A and B. The kidney data have been omitted from B, enabling a smaller %ID/g scale and closer examination of the data.

ecules. Investigations with the anti-CEA diabody reported a $T_{1/2\alpha}$ of 0.25 ± 0.02 h and $T_{1/2\beta}$ of 2.89 ± 0.74 h (18), whereas the anti-HER2/neu ¹²⁵I-labeled C6.5 diabody displayed a $T_{1/2\alpha}$ of 0.67 h and a $T_{1/2\beta}$ of 6.42 h (30). The pharmacokinetic profile

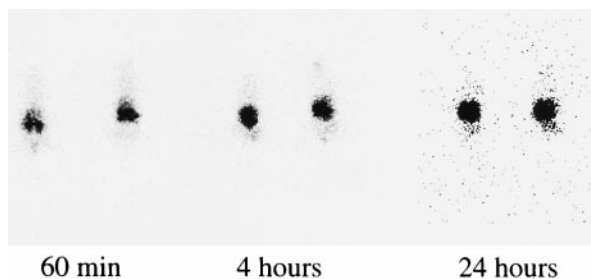


Fig. 7 Whole body gamma camera images of ¹¹¹In-CHX-A''-DTPA hu3S193 diabody in BALB/c mice bearing s.c. MCF-7 tumors on the left flank (right side of mouse image) and SW1222 control tumors on the right flank (left side of mouse image). Dorsal images were taken at 1 h (*n* = 2), 4 h, (*n* = 2), and 24 h (*n* = 2), after injection of radiolabeled construct with the mice supine on the gamma camera. The radioactivity seen in the middle of each image corresponds to kidney uptake.

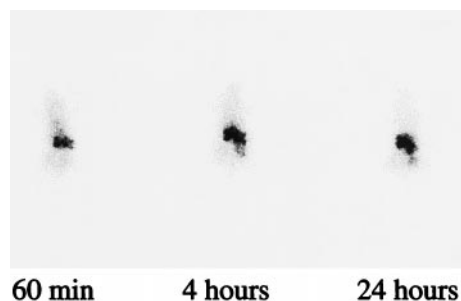


Fig. 8 Whole body gamma camera images of ¹¹¹In-CHX-A''-DTPA hu3S193 F(ab')₂ in BALB/c mice bearing s.c. MCF-7 tumors on the left flank (right side of mouse image) and SW1222 control tumors on the right flank (left side of image). Dorsal images were taken at 1 h (*n* = 1), 4 h, (*n* = 1), and 24 h (*n* = 1), after injection of radiolabeled construct with the mice supine on the gamma camera. The radioactivity seen in the middle of each image corresponds to kidney uptake.

of the anti-CEA diabody very closely resembles the profile observed for the ¹¹¹In diabody (*T*_{1/2α}, 0.45 h; *T*_{1/2β}, 2.7 h). Investigations with an ¹³¹I-labeled anti-CEA F(ab')₂ observed a *T*_{1/2} of 12 h (46), which compares favorably with the pharmacokinetic results of the ¹¹¹In-labeled hu3S193 F(ab')₂ (*T*_{1/2α}, 1.76 h; *T*_{1/2β}, 12.6 h). The pharmacokinetic profiles observed are typical of antibody-based molecules with sizes above the renal threshold for first-pass clearance.

The tissue biodistribution and gamma camera images for both conjugates showed prominent kidney uptake because of the clearance of the constructs and greater retention of the ¹¹¹In metabolite in the renal system (Figs. 5–8). Localization of radiolabeled conjugates to other normal tissues investigated was nonspecific and attributable to blood pool activity. The uptake of small molecular weight constructs in the kidney presents an obstacle for therapy studies because it may result in potentially greater renal toxicity (47). Therefore, experiments aimed at blocking kidney uptake by the pretreatment or coadministration of cationic amino acids, such as D-lysine with radiolabeled antibody conjugates, which have been shown to reduce kidney uptake, need to be assessed (48, 49). Further improvements in pharmacokinetics can be achieved by increasing the surface

negative charge or modifying the radionuclide chemistry, both strategies for reducing the renal uptake observed frequently in small engineered antibodies (49, 50).

Dimer molecules similar to the hu3S193 diabody are also useful reagents for delivering radioisotope to tumors and, similar to diabodies, are potentially most useful for imaging and immunodiagnosis because of their rapid clearance from the circulation (51, 52). However, theoretically, diabodies (*M*_r 60,000) will be more stable than scFv dimers, and because diabodies also provide more rapid tumor penetration and clearance than F(ab')₂ (*M*_r 100,000), they may therefore be the preferred reagent for radioimaging with short half-life radionuclides such as ^{99m}Tc and ¹²³I (gamma emitters) or ¹⁸F (positron emitter; Ref. 38). Conversely, for longer half-life radiolabels designed for immunotherapy (e.g., ⁹⁰Y and ¹³¹I), the slower blood clearance of F(ab')₂ compared with diabodies generates a higher tumor: blood ratio, higher total tumor uptake, and higher radiotherapeutic index. Following this trend, we would expect that larger multivalent radiolabeled triabodies (*M*_r 90,000) and tetrabodies (*M*_r 120,000) would outperform diabodies in total tumor uptake because of higher avidity and slower blood clearance (12, 48), which makes these constructs attractive for further development and evaluation. The hu3S193 F(ab')₂ showed a high maximal tumor uptake and is an interesting molecule to pursue in therapeutic studies, possibly in combination with other antibody constructs, targeting different tumor compartments, including the stroma and vasculature. The optimal construct size is therefore one that balances the rapidity of blood clearance, the absolute tumor uptake, and the tumor: blood ratios for the desired diagnostic or therapeutic application.

ACKNOWLEDGMENTS

We thank Angela J. Mountain, Angela Rigopoulos, and Cathrine M. Hall for technical advice and their support with the FPLC analysis, cell binding assays, and animal handling, respectively.

REFERENCES

- Smith, G., and Henderson, I. C. New treatments for breast cancer. *Semin. Oncol.*, 23: 506–528, 1996.
- Henderson, I. C., Garber, J. E., Breitmeyer, J. B., Hayes, D. F., and Harris, J. R. Comprehensive management of disseminated breast cancer. *Cancer (Phila.)*, 66: 1439–1448, 1990.
- De Vita, V. T., Hellman, S., and Rosenberg, S. A. Principles of chemotherapy. In: V. T. De Vita, S. Hellman, and S. A. Rosenberg (eds.), *Cancer: Principles and Practices of Oncology*, pp. 257–286. Philadelphia: J. B. Lippincott Co., 1985.
- Scott, A. M., and Cebon, J. Clinical promise of tumor immunology. *Lancet*, 349 (Suppl. 2): S119–22, 1997.
- van den Eynde, J., and Scott, A. M. (eds.). *Tumor Antigens. Encyclopedia of Immunology*, Ed. 2, pp. 2424–2431. London: Academic Press, Ltd., 1998.
- Kim, Y. S., Yuan, M., Itzkowitz, S. H., Sun, Q. B., Kaizu, T., Palekar, A., Trump, B. F., and Hakomori, S. Expression of LeY and extended LeY blood group-related antigens in human malignant, pre-malignant, and nonmalignant colonic tissues. *Cancer Res.*, 46: 5985–5992, 1986.
- Lloyd, K. O. Philip Levine award lecture. Blood group antigens as markers for normal differentiation and malignant change in human tissues. *Am. J. Clin. Pathol.*, 87: 129–139, 1987.
- Zhang, S., Zhang, H. S., Cordon-Cardo, C., Reuter, V. E., Singhal, A. K., Lloyd, K. O., and Livingston, P. O. Selection of tumor antigens

- as targets for immune attack using immunohistochemistry. II. Blood group-related antigens. *Int. J. Cancer*, 73: 50–56, 1997.
9. Sakamoto, J., Furukawa, K., Cordon-Cardo, C., Yin, B. W., Rettig, W. J., Oettgen, H. F., Old, L. J., and Lloyd, K. O. Expression of Lewis^a, Lewis^b, X, and Y blood group antigens in human colonic tumors and normal tissue and in human tumor-derived cell lines. *Cancer Res.*, 46: 1553–1561, 1986.
 10. Kitamura, K., Stockert, E., Garin-Chesa, P., Welt, S., Lloyd, K. O., Armour, K. L., Wallace, T. P., Harris, W. J., Carr, F. J., and Old, L. J. Specificity analysis of blood group Lewis-y (Le(y)) antibodies generated against synthetic and natural Le(y) determinants. *Proc. Natl. Acad. Sci. USA*, 91: 12957–12961, 1994.
 11. Scott, A. M., Geleick, D., Rubira, M., Clarke, K., Nice, E. C., Smyth, F. E., Stockert, E., Richards, E. C., Carr, F. J., Harris, W. J., Armour, K. L., Rood, J., Kypridis, A., Kronina, V., Murphy, R., Lee, F. T., Liu, Z., Kitamura, K., Ritter, G., Laughton, K., Hoffman, E., Burgess, A. W., and Old, L. J. Construction, production, and characterization of humanized anti-Lewis Y monoclonal antibody 3S193 for targeted immunotherapy of solid tumors. *Cancer Res.*, 60: 3254–3261, 2000.
 12. Hudson, P. J., and Kortt, A. A. High avidity scFv multimers: diabodies and triabodies. *J. Immunol. Methods*, 231: 177–189, 1999.
 13. Hudson, P. J. Recombinant antibody constructs in cancer therapy. *Curr. Opin. Immunol.*, 11: 548–557, 1999.
 14. Hayden, M. S., Gilliland, L. K., and Ledbetter, J. A. Antibody engineering. *Curr. Opin. Immunol.*, 9: 201–212, 1997.
 15. Colcher, D., Goel, A., Pavlinkova, G., Beresford, G., Booth, B., and Batra, S. K. Effects of genetic engineering on the pharmacokinetics of antibodies. *Q. J. Nucl. Med.*, 43: 132–139, 1999.
 16. Burrows, F. J., and Thorpe, P. E. Vascular targeting—a new approach to the therapy of solid tumors. *Pharmacol. Ther.*, 64: 155–174, 1994.
 17. Adams, G. P., and Schier, R. Generating improved single-chain Fv molecules for tumor targeting. *J. Immunol. Methods*, 231: 249–260, 1999.
 18. Wu, A. M., Williams, L. E., Zieran, L., Padma, A., Sherman, M., Bebb, G. G., and Odom-Maryon, T. Anticarcinoembryonic antigen (CEA) diabody for rapid tumor targeting and imaging. *Tumor Targeting*, 4: 47–54, 1999.
 19. Pedley, R. B., Boden, J. A., Boden, R., Dale, R., and Begent, R. H. Comparative radioimmunotherapy using intact or F(ab')₂ fragments of ¹³¹I anti-CEA antibody in a colonic xenograft model. *Br. J. Cancer*, 68: 69–73, 1993.
 20. Soule, H. D., Vazquez, J., Long, A., Albert, S., and Brennan, M. A human cell line from a pleural effusion derived from a breast carcinoma. *J. Natl. Cancer Inst.*, 51: 1409–1416, 1973.
 21. Atwell, J. L., Breheny, K. A., Lawrence, L. J., McCoy, A. J., Kortt, A. A., and Hudson, P. J. scFv multimers of the antineuraminidase antibody NC10: length of the linker between VH and VL domains dictates precisely the transition between diabodies and triabodies. *Protein Eng.*, 12: 597–604, 1999.
 22. Power, B. E., and Hudson, P. J. Synthesis of high avidity antibody fragments (scFv multimers) for cancer imaging. *J. Immunol. Methods*, 242: 193–204, 2000.
 23. Wu, C., Kobayashi, H., Sun, B., Yoo, T. M., Paik, C. H., Gansow, O. A., Carrasquillo, J. A., Pastan, I., and Brechbiel, M. W. Stereochemical influence on the stability of radio-metal complexes *in vivo*. Synthesis and evaluation of the four stereoisomers of 2-(p-nitrobenzyl)-trans-CyDTPA. *Bioorg. Med. Chem.*, 5: 1925–1934, 1997.
 24. Hunter, W. M., and Greenwood, F. C. Preparation of iodine-131 labeled growth hormone of high specific radioactivity. *Nature (Lond.)*, 194: 495–496, 1962.
 25. Lindmo, T., Boven, E., Cuttitta, F., Fedorko, J., and Bunn, P. A., Jr. Determination of the immunoreactive fraction of radiolabeled monoclonal antibodies by linear extrapolation to binding at infinite antigen excess. *J. Immunol. Methods*, 72: 77–89, 1984.
 26. Clarke, K., Lee, F. T., Brechbiel, M. W., Smyth, F. E., Old, L. J., and Scott, A. M. *In vivo* biodistribution of a humanized anti-Lewis Y monoclonal antibody (hu3S193) in MCF-7 xenografted BALB/c nude mice. *Cancer Res.*, 60: 4804–4811, 2000.
 27. Co, M. S., Baker, J., Bednarik, K., Janzek, E., Neruda, W., Mayer, P., Plot, R., Stumper, B., Vasquez, M., Queen, C., and Loibner, H. Humanized anti-Lewis Y antibodies: *in vitro* properties and pharmacokinetics in rhesus monkeys. *Cancer Res.*, 56: 1118–1125, 1996.
 28. Holliger, P., Prospero, T., and Winter, G. “Diabodies”: small bivalent and bispecific antibody fragments. *Proc. Natl. Acad. Sci. USA*, 90: 6444–6448, 1993.
 29. Hudson, P. J. Recombinant antibody fragments. *Curr. Opin. Biotechnol.*, 9: 395–402, 1998.
 30. Adams, G. P., Schier, R., McCall, A. M., Crawford, R. S., Wolf, E. J., Weiner, L. M., and Marks, J. D. Prolonged *in vivo* tumor retention of a human diabody targeting the extracellular domain of human HER2/neu. *Br. J. Cancer*, 77: 1405–1412, 1998.
 31. Buchegger, F., Pelegrin, A., Delaloye, B., Bischof-Delaloye, A., and Mach, J. P. Iodine-131-labeled MAb F(ab')₂ fragments are more efficient and less toxic than intact anti-CEA antibodies in radioimmunotherapy of large human colon carcinoma grafted in nude mice. *J. Nucl. Med.*, 31: 1035–1044, 1990.
 32. Adams, G. P., Schier, R., Marshall, K., Wolf, E. J., McCall, A. M., Marks, J. D., and Weiner, L. M. Increased affinity leads to improved selective tumor delivery of single-chain Fv antibodies. *Cancer Res.*, 58: 485–490, 1998.
 33. Bera, T. K., and Pastan, I. Comparison of recombinant immunotoxins against LeY antigen expressing tumor cells: influence of affinity, size, and stability. *Bioconj. Chem.*, 9: 736–743, 1998.
 34. Viti, F., Tarli, L., Giovannoni, L., Zardi, L., and Neri, D. Increased binding affinity and valence of recombinant antibody fragments lead to improved targeting of tumoral angiogenesis. *Cancer Res.*, 59: 347–352, 1999.
 35. Nikula, T. K., Curcio, M. J., Brechbiel, M. W., Gansow, O. A., Finn, R. D., and Scheinberg, D. A. A rapid, single vessel method for preparation of clinical grade ligand conjugated monoclonal antibodies. *Nucl. Med. Biol.*, 22: 387–390, 1995.
 36. Griffin, T. W., Brill, A. B., Stevens, S., Collins, J. A., Bokhari, F., Bushe, H., Stochl, M. C., Gionet, M., Rusckowski, M., Stroupe, S. D., *et al.* Initial clinical study of indium-111-labeled clone 110 anticarcinoembryonic antigen antibody in patients with colorectal cancer. *J. Clin. Oncol.*, 9: 631–640, 1991.
 37. Pietersz, G. A., Patrick, M. R., and Chester, K. A. Preclinical characterization and *in vivo* imaging studies of an engineered recombinant technetium-99m-labeled metallothionein-containing anticarcinoembryonic antigen single-chain antibody. *J. Nucl. Med.*, 39: 47–56, 1998.
 38. Yorke, E. D., Beaumier, P. L., Wessels, B. W., Fritzberg, A. R., and Morgan, A. C., Jr. Optimal antibody-radionuclide combinations for clinical radioimmunotherapy: a predictive model based on mouse pharmacokinetics. *Int. J. Radiat. Appl. Instrum. Part B*, 18: 827–835, 1991.
 39. Adams, G. P., Shaller, C. C., Chappell, L. L., Wu, C., Horak, E. M., Simmons, H. H., Litwin, S., Marks, J. D., Weiner, L. M., and Brechbiel, M. W. Delivery of the α -emitting radioisotope bismuth-213 to solid tumors via single-chain Fv and diabody molecules. *Nucl. Med. Biol.*, 27: 339–346, 2000.
 40. Hu, S., Shively, L., Raubitschek, A., Sherman, M., Williams, L. E., Wong, J. Y., Shively, J. E., and Wu, A. M. Minibody. A novel engineered anticarcinoembryonic antigen antibody fragment (single-chain Fv-CH3) which exhibits rapid, high-level targeting of xenografts. *Cancer Res.*, 56: 3055–3061, 1996.
 41. King, D. J., Turner, A., Farnsworth, A. P., Adair, J. R., Owens, R. J., Pedley, R. B., Baldock, D., Proudfoot, K. A., Lawson, A. D., Beeley, N. R., *et al.* Improved tumor targeting with chemically cross-linked recombinant antibody fragments. *Cancer Res.*, 54: 6176–6185, 1994.

42. Garrigues, J., Garrigues, U., Hellstrom, I., and Hellstrom, K. E. Ley specific antibody with potent antitumor activity is internalized and degraded in lysosomes. *Am. J. Pathol.*, *142*: 607–622, 1993.
43. Mariani, G., Kassis, A. I., and Adelstein, S. J. Antibody internalization by tumor cells: implications for tumor diagnosis and therapy. *J. Nucl. Med. Allied Sci.*, *34*: 51–54, 1990.
44. Brown, B. A., Comeau, R. D., Jones, P. L., Liberatore, F. A., Neacy, W. P., Sands, H., and Gallagher, B. M. Pharmacokinetics of the monoclonal antibody B72.3 and its fragments labeled with either ¹²⁵I or ¹¹¹In. *Cancer Res.*, *47*: 1149–1154, 1987.
45. Vogel, C. A., Bischof-Delaloye, A., Mach, J. P., Pelegrin, A., Hardman, N., Delaloye, B., and Buchegger, F. Direct comparison of a radioiodinated intact chimeric anti-CEA MAb with its F(ab')₂ fragment in nude mice bearing different human colon cancer xenografts. *Br. J. Cancer*, *68*: 684–690, 1993.
46. Buchegger, F., Pfister, C., Fournier, K., Prevel, F., Schreyer, M., Carrel, S., and Mach, J. P. Ablation of human colon carcinoma in nude mice by ¹³¹I-labeled monoclonal anticarcinoembryonic antigen antibody F(ab')₂ fragments. *J. Clin. Investig.*, *83*: 1449–1456, 1989.
47. Dillman, R. O. Monoclonal antibodies for treating cancer. *Ann. Intern. Med.*, *111*: 592–603, 1989.
48. Behr, T. M., Sharkey, R. M., Sgouros, G., Blumenthal, R. D., Dunn, R. M., Kolbert, K., Griffith, G. L., Siegel, J. A., Becker, W. S., and Goldenberg, D. M. Overcoming the nephrotoxicity of radiometal-labeled immunoconjugates: improved cancer therapy administered to a nude mouse model in relation to the internal radiation dosimetry. *Cancer (Phila.)*, *80*: 2591–2610, 1997.
49. Arano, Y., Fujioka, Y., Akizawa, H., Ono, M., Uehara, T., Wakisaka, K., Nakayama, M., Sakahara, H., Konishi, J., and Saji, H. Chemical design of radiolabeled antibody fragments for low renal radioactivity levels. *Cancer Res.*, *59*: 128–134, 1999.
50. Pavlinkova, G., Beresford, G., Booth, B. J., Batra, S. K., and Colcher, D. Charge-modified single chain antibody constructs of monoclonal antibody CC49: generation, characterization, pharmacokinetics, and biodistribution analysis. *Nucl. Med. Biol.*, *26*: 27–34, 1999.
51. Pavlinkova, G., Booth, B. J., Batra, S. K., and Colcher, D. Radioimmunotherapy of human colon cancer xenografts using a dimeric single-chain Fv antibody construct. *Clin. Cancer Res.*, *5*: 2613–2619, 1999.
52. Beresford, G. W., Pavlinkova, G., Booth, B. J., Batra, S. K., and Colcher, D. Binding characteristics and tumor targeting of a covalently linked divalent CC49 single-chain antibody. *Int. J. Cancer*, *81*: 911–917, 1999.